Catalytic Fluorination by Halide Exchange with 16-Electron Ruthenium(II) Complexes. X-ray Structure of $[Tl(\mu\text{-}F)_2Ru(dppe)_2]PF_6$

Peter Barthazy, Antonio Togni,* and Antonio Mezzetti*

Laboratory of Inorganic Chemistry, Swiss Federal Institute of Technology, ETH Zentrum, CH-8092 Zürich, Switzerland

Received April 6, 2001

The 16-electron ruthenium(II) complexes $[RuCl(dppe)_2]PF_6$ (**2**; dppe = 1,2-bis(diphenylphosphino)ethane), $[RuCl(chiraphos)_2]PF_6$ (**3**; chiraphos = (*S,S*)-3,4-bis(diphenylphosphino)butane), and [RuCl(PNNP)]PF_6 (**4**; PNNP = (1*S*,2*S*)-*N*,*N*′-bis[2-(diphenylphosphino)-benzylidene]diaminocyclohexane) catalyze the nucleophilic fluorination of activated alkyl halides with a catalyst loading as low as 1 mol %. The alkyl halides $(CH_3)_3CX$ (X = Br, **5c**; X = I, **5d**), Ph_2CHBr (**6c**), and PhCH(Me)Br (**7c**) are converted to the fluoro analogues in the presence of TlF as the fluoride source. Yields are between 31 and 83%. The chiral complex **4** converts **7c** to PhCH(Me)F (**7a**) with 49% yield after 24 h. At 1% conversion, **7a** is nonracemic (16% ee), which indicates that kinetic resolution occurs, albeit at a low level. The fluorination of 1,2-dibromo-1,2,3,4-tetrahydronaphthalene (**8c**) is highly regioselective and gives 1-fluoro-2-bromo-1,2,3,4-tetrahydronaphthalene (**8a**) in 68% yield. The difluoro-bridged thallium adduct $[Tl(\mu\text{-}F)_2Ru(dppe)_2]PF_6$ (**9**) was observed by ^{31}P NMR during catalysis with **2** and independently prepared by reaction of **2** with TlF (2 equiv). Complex **9** was characterized by ^{1}H, ^{31}P, ^{19}F, and ^{205}Tl NMR spectroscopy, as well as by X-ray diffraction.

Introduction

The use of transition-metal complexes as catalysts for reaction where a new carbon−fluorine bond is formed is still exceedingly rare, despite the importance of, for example, organofluorine compounds in medicinal chemistry.[1] One of us recently reported the first enantioselective electrophilic fluorination of β-keto esters by the N−F reagent F-TEDA catalyzed by Ti(TADDOLato) complexes.[2] While this reaction appears to proceed via the formation of a coordinated substrate enolate that is subsequently attacked by the N−F reagent, a direct interaction between the metal and the fluorine atom to be transferred is not required. Similarly, in the recently reported first asymmetric ring opening of epoxides by hydrofluorinating agents catalyzed by Jacobsen's chiral [CrCl(salen)] complexes, the involvement of fluorochromium species was considered as very improbable.[3]

In contrast to this, a variety of well-defined metal fluoro complexes, low-valent fluoride salts,[4] or high-valent metal fluorides and oxofluorides[5] have been shown to act as fluoride transfer agents in stoichiometric reactions, in particular with alkyl, acyl, and silyl halides. A recent example is the stoichiometric reaction of $[PdF(Ph)(PPh_3)_2]$ with CH_2Cl_2 to give CH_2ClF and CH_2F_2.[6] A further example of stoichiometric fluorination has recently been reported from our laboratories and involves the 16-electron ruthenium(II) complex $[RuF(dppp)_2]^+$ (**1c**; dppp = 1,3-bis(diphenylphosphino)ethane), obtained by reaction of the well-known chloro analogue[7] with TlF (Scheme 1a).[8a] Complex **1c** reacts, in fact, with tertiary alkyl halides to give the corresponding R−F derivatives (Scheme 1b).[8]

We now find that the X/F exchange (X = Br, I) in the organic molecule can be combined with the halide metathesis of $[RuX(dppp)_2]^+$. The resulting catalytic reaction exploits TlF as the fluoride source and five-coordinate ruthenium complexes as catalysts. Among these complexes, there are 16-electron species of general formula $[RuClP_2L_2]^+$ (L = P or N donor) that we have recently used as catalysts for the epoxidation and cyclopropanation of olefins (Chart 1).[9]

* To whom correspondence should be addressed. E-mail: A.T., togni@inorg.chem.ethz.ch; A.M., mezzetti@inorg.chem.ethz.ch.

(1) See, for instance: (a) Davis, F. A.; Qi, H.; Sundarababu, G. In *Enantiocontrolled Synthesis of Fluoro-Organic Compounds*; Soloshonok, V. A., Ed.; Wiley: New York, 1999; p 1. (b) Hoffman, R. V.; Tao, J. In *Asymmetric Fluoroorganic Chemistry*; Ramachandran, P. V., Ed.; ACS Symposium Series 746; American Chemical Society: Washington, DC, 2000; p 52. (c) Hiyama, T. In *Organofluorine Compounds*; Yamamoto, H., Ed.; Springer: Berlin, 2000; p 137.

(2) Hintermann, L.; Togni, A. *Angew. Chem., Int. Ed.* **2000**, *39*, 4359.

(3) Bruns, S.; Haufe, G. *J. Fluorine Chem.* **2000**, *104*, 247.

(4) Taverner, S. J.; Heath, P. A.; Clark, J. H. *New J. Chem.* **1998**, 655 and references therein.

(5) (a) Dukat, W. W.; Holloway, J. H.; Hope, E. G.; Rieland, M. R.; Townson, P. J.; Powell, R. L. *J. Chem. Soc., Chem. Commun.* **1993**, 1429. (b) Holloway, J. H.; Hope, E. G.; Townson, P. J.; Powell, R. L. *J. Fluorine Chem.* **1996**, *76*, 105.

(6) Grushin, V. V. *Angew. Chem., Int. Ed. Engl.* **1998**, *37*, 994. See also: Fraser, S. L.; Antipin, M. Y.; Khroustslyov, V. N.; Grushin, V. V. *J. Am. Chem. Soc.* **1997**, *119*, 4769. Pilon, M. C.; Grushin, V. V. *Organometallics* **1998**, *17*, 1774.

(7) Bressan, M.; Rigo, P. *Inorg. Chem.* **1975**, *14*, 2286.

(8) (a) Barthazy, P.; Hintermann, L.; Stoop, R. M.; Wörle, M.; Mezzetti, A.; Togni, A. *Helv. Chim. Acta* **1999**, *82*, 2448. (b) Barthazy, P.; Stoop, R. M.; Wörle, M.; Togni, A.; Mezzetti, A. *Organometallics* **2000**, *19*, 2844.

(9) (a) Stoop, R. M.; Bauer, C.; Setz, P.; Wörle, M.; Wong, T. Y. H.; Mezzetti, A. *Organometallics* **1999**, *18*, 5691. (b) Stoop, R. M.; Mezzetti, A. *Green Chem.* **1999**, 39. (c) Stoop, R. M.; Bachmann, S.; Valentini, M.; Mezzetti, A. *Organometallics* **2000**, *19*, 4117. (d) Bachmann, S.; Furler, M.; Mezzetti, A. *Organometallics* **2001**, *20*, 2102.

10.1021/om010288g CCC: $20.00
Publication on Web 07/10/2001

Scheme 1

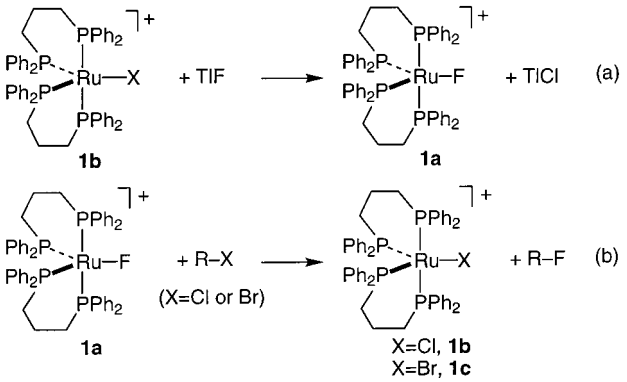

Chart 1

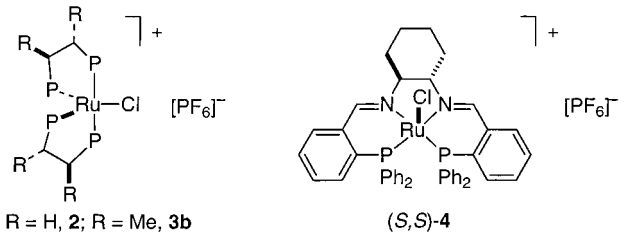

Scheme 2

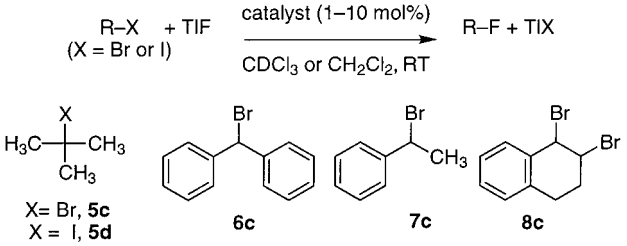

Results and Discussion

The catalytic fluorination is depicted in Scheme 2, together with the substrates used. Conditio sine qua non for the success of the fluorination is that the reaction solutions be protected from adventitious water and from the contact with glass surfaces. Two methods were developed. Small-scale reactions were run in an NMR tube fitted with a Young valve and a Teflon insert, which was shaken mechanically during the reaction time (method A). Solution reactions were prepared in a glovebox under purified nitrogen (see Experimental Section). On a larger scale, the reaction solutions were prepared and kept in Teflon vessels in a glovebox and stirred magnetically (method B).

We started our investigation with *tert*-butyl bromide (**5c**) as substrate and [RuCl(dppp)$_2$]PF$_6$ (**1b**)[7] (10 mol %) as the catalyst precursor. Owing to the low boiling point of **5a** (13 °C), the reaction was carried out in an NMR tube fitted with a Young valve. The reaction of *tert*-butyl bromide (**5c**) with TlF in the presence of **1b** is very slow at room temperature. Raising the temperature to 50 °C accelerates the reaction, and 42% conversion of **5c** is obtained after 12 h (Table 1, run 1). However, the main product is isobutene (15%), deriving from the elimination of HBr, and the yield of *tert*-butyl fluoride (**5a**) is as low as 2%. The formation of (Bu^t)$_2$O (10% of starting **5c**) suggests that adventitious water cannot be removed completely although precautions are taken (see Experimental Part). A control reaction, run without adding complex **1b**, showed that *tert*-butyl bromide does not react with TlF under these conditions.

Next, we investigated the related complex [RuCl(dppe)$_2$]$^+$ (**2**; dppe = 1,2-bis(diphenylphosphino)ethane), which was recently reported by Morris.[10] In the presence of **2** as catalyst (10 mol %), *tert*-butyl bromide (**5c**) reacted at room temperature with TlF (1.1 equiv) to yield *tert*-butyl fluoride (**5a**, 60% yield). Some isobutene (ca. 30%) was also formed (Table 1, run 2). The use of *tert*-butyl iodide (**5d**) substantially inhibits the elimination reaction, speeds up the reaction, and improves the yield of *tert*-butyl fluoride (run 3). The chiral analogue [RuCl(chiraphos)$_2$]PF$_6$ (**3**; chiraphos = (*S*,*S*)-3,4-bis(diphenylphosphino)butane)[9a] gives similar results with a catalyst loading of only 2 mol % (run 3). In the presence of the dppe derivative **2**, the benzylic bromide 1-bromo-1,1-diphenylmethane (**6c**) gave the fluoro derivative Ph$_2$CHF (**6a**) in high yield after 24 h of reaction time (run 5).

Having chiral catalysts at our disposal, we tested racemic 1-bromo-1-phenylethane (**7c**) as substrate. With the (achiral) dppe derivative **2**, **7c** is fluorinated with moderate efficiency (runs 6 and 7). In particular, the catalyst loading can be reduced to 1 mol % without a major loss in the yield and selectivity, but at the cost of longer reaction times. The chiraphos derivative **3** is more active and selective than **2** (run 8). However, GC analysis on a chiral column indicated that racemic 1-phenyl-1-fluoroethane (**7a**) is formed.

Thus, we tested the recently reported five-coordinate complex [RuCl(PNNP)]PF$_6$ (**4**; PNNP = (1*S*,2*S*)-*N*,*N*′-bis[2-diphenylphosphino)benzylidene]diaminocyclohexane).[9b−d] Complex **4** gave **7a** in moderate yield (49%, run 9). More importantly, monitoring of the enantiomeric excess of 1-phenyl-1-fluoroethane by GC during the reaction indicated that the initially formed product is nonracemic (Table 2). At 1% conversion, the enantiomeric excess of **7a** is 16% ee, as measured by GC on a chiral column. The enantiomeric excess drops with longer reaction times and reaches 3% at 100% conversion after 24 h of reaction time. As several measurements of the enantiomeric excess of the products obtained with achiral **2** (as well as with chiral **3**) gave 0 ± 0.1% ee, it is reasonable to assume a 3% ee as significant.

The above data suggest that kinetic resolution of *rac*-**7c** occurs to some extent. Possible mechanisms encompass classic kinetic resolution (if an S$_N$2 mechanism is operative) or dynamic kinetic resolution.[11] In the latter case, fast racemization of the substrate would occur, most probably due to an S$_N$1 mechanism. Thus, the enantiomeric excess of the unreacted substrate should give an indication as to which mechanism occurs. Unfortunately, we were not able to determine the enantiomeric excess of **7c** by means of GC on a chiral column.

(10) Chin, B.; Lough, A. J.; Morris, R. H.; Schweitzer, C. T.; D'Agostino, C. *Inorg. Chem.* **1994**, *33*, 6278.
(11) See, for instance: Keith, J. M.; Larrow, J. F.; Jacobsen, E. N. *Adv. Synth. Catal.* **2001**, *343*, 5 and ref 9 therein.

Table 1. Catalytic Fluorination[a]

run	cat.	substrate	mol %	method	*t* (days)	conversn (%)	yield (%) R−F	yield (%) ether	yield (%) olefin
1[b]	**1b**	**5c**	10	a	0.5	42	2	10	15
2	**2**	**5c**	10	a	5	100	63	9	28
3	**2**	**5d**	10	a	0.2	100	84	8	8
4	**3**	**5c**	2	a	5	94	57	7	31
5	**2**	**6c**	10	a	1	93	83	2	
6	**2**	**7c**	10	a	4	51	31	3	nd
7	**2**	**7c**	1	b	8	53	34	nd	nd
8	**3**	**7c**	1	b	2	86	76	nd	nd
9	**4**	**7c**	1	b	1	100	49	nd	nd
10	**4**	**8c**	10	a	3	94	68	*c*	traces

[a] Control reactions under the same conditions but without the catalyst showed no reaction for **5c** and **8c**, 6% conversion (6% yield) for **5d**, 2% (1%) for **6c**, and 13% (7%) for **7c**. The abbreviation nd means not determined. [b] At 50 °C. [c] Unknown byproducts.

Table 2. Conversion, Yield, and Enantiomeric Excess of 7a as a Function of Reaction Time during the Fluorination Catalyzed by 4[a]

t (h)	conversn (%)	yield (%)	ee (%)
1	1	1	16
2	28	4	13
4	31	10	7
6	43	19	2
24	quant	62	3

[a] Portions of the reaction solution was periodically sampled and analyzed by GC (see Experimental Section).

Finally, *trans*-1,2-dibromo-1,2,3,4-tetrahydronaphthalene (**8c**) was fluorinated regio- and stereoselectively at the C(1) position in the presence of **2** (10 mol %) (run 10). The reaction gave *trans*-1-fluoro-2-bromo-1,2,3,4-tetrahydronaphthalene as the major product (68% yield) after 3 days. The elimination product (1,2-dihydronaphthalene) is present in traces, along with yet unidentified products. The retention of configuration at C(1) in the reaction of **8c** can be explained by a neighboring-group mechanism, that is, involving the rate-determining formation of a bromonium intermediate. This would exclude, at least in this case, an S_N2 mechanism.

Other substrates did not react (or reacted very sluggishly) under the conditions described above. In particular, primary alkyl halides, such as 2-iodopropane and cyclohexyl bromide, are completely unreactive. The fact that the reactivity is higher with typical S_N1 substrates suggests that substantial charge separation is involved in the transition state of the halogen transfer reaction. A further limitation is the poor tolerance for functional groups. Protic substrates, such as alcohols and carboxylic acids, do not react owing to the formation of HF. Also, α-halogeno ketones are unreactive.

The catalytic system described herein requires shorter reaction times and milder conditions than those of traditional methods employing fluoride salts, such as biphasic fluorination with spray-dried KF or phase-transfer agents.[12] Thus, nearly quantitative conversions and selectivities up to 88% for the fluorinated products are obtained. The present system also reacts with less activated haloalkanes than required by silver and copper florides.[13] Moreover, kinetic resolution takes place, albeit with a low efficiency, as racemic **6a** gives slightly enantiomerically enriched Ph(Me)CHF in the reaction with the chiral catalyst **2**. This is an additional indication that a ruthenium complex is involved in the key step of the X/F exchange (probably halide abstraction from the substrate) and not only as phase-transfer agent and bromide (or iodide) scavenger.

$[Tl(\mu\text{-}F)_2Ru(dppe)_2]PF_6$. Monitoring of the (yellow) catalytic solutions by means of ^{31}P NMR spectroscopy showed that the doubly fluoro-bridged TlF adduct $[Tl(\mu\text{-}F)_2Ru(dppe)_2]PF_6$ (**9**) is the only detectable metal-containing species in the reaction catalyzed by $[RuCl(dppe)_2]PF_6$ (**2**). We independently prepared **9** by reaction of **2** with TlF (2 equiv). The yellow solid was isolated from the CH_2Cl_2 solutions by precipitation with 2-propanol. The presence of the P_4RuF_2Tl unit is strongly suggested by the AA′MM′QQ′X spin system observed in the ^{19}F, ^{31}P, and ^{205}Tl NMR spectra. The spectra are not well-resolved (either in $CDCl_3$ or in CH_2Cl_2), probably due to a dynamic process that is fast at room temperature. Lowering the temperature (in CD_2Cl_2 solution) improves the resolution only in the case of the ^{31}P NMR spectrum. However, the pattern observed is unambiguous. The ^{19}F spectrum (20 °C) consists of a broad doublet of doublets at δ −296 with a $^1J_{Tl,F}$ coupling constant of ca. 800 Hz. The signals are broad, owing to the nonresolved coupling to the ^{203}Tl and ^{205}Tl isotopomers (29.5 and 70.5% abundance, respectively). The same value of the $^1J_{Tl,F}$ coupling constant is observed for the broad triplet at δ 1055 in the ^{205}Tl NMR spectrum (20 °C), which arises from the coupling to the two (chemically equivalent) F nuclei. The room-temperature ^{31}P NMR spectrum consists of the AA′MM′ part of the spin system, which features overlapping signals for the two pairs of chemically equivalent P atoms. However, the chemical shifts of the P_A, $P_{A'}$ and P_M, $P_{M'}$ atoms shift differently upon lowering the temperature. Thus, resolved signals are observed at −90 °C, that is, a *pseudo*-quintet at δ 55.7 for the axial P atoms ($J_{P,P'} \cong$ 19 Hz, $J_{P,F} \simeq$ 19 Hz), and a doublet of triplets at δ 54.4 for the equatorial ones. The attribution of the latter signal to the equatorial phosphines is based on the large apparent $J_{P,F}$ coupling constant of 146 Hz, which is the sum $J_{P,F} + J_{P,F'}$, the trans and cis P−Ru−F coupling constants. The $J_{P,F} + J_{P,F'}$ coupling constant is detected also in the ^{31}P-coupled ^{19}F NMR spectrum. The ^{31}P-decoupled ^{19}F NMR spectrum shows only the doublet due to the coupling to thallium.

An X-ray study supports the formulation of **9** (Figure 1, Table 3). The complex cation is approximately C_2 symmetric with a *pseudo*-binary axis through the Ru and Tl atoms. As a consequence, the $Ru(\mu\text{-}F)_2Tl$ ring is symmetrical and planar within ±0.026 Å. The Ru−F

(12) Rock, M. H. *Methoden Organische Chemie (Houben-Weyl)*, 4th ed.; Thieme: Stuttgart, Germany, 1986; Vol. E10b/1, pp 50−65.
(13) Yoneda, N.; Fukukara, T.; Yamagishi, K.; Suzuki, A. *Chem. Lett.* **1987**, 1675. See also ref 1b, p 192.

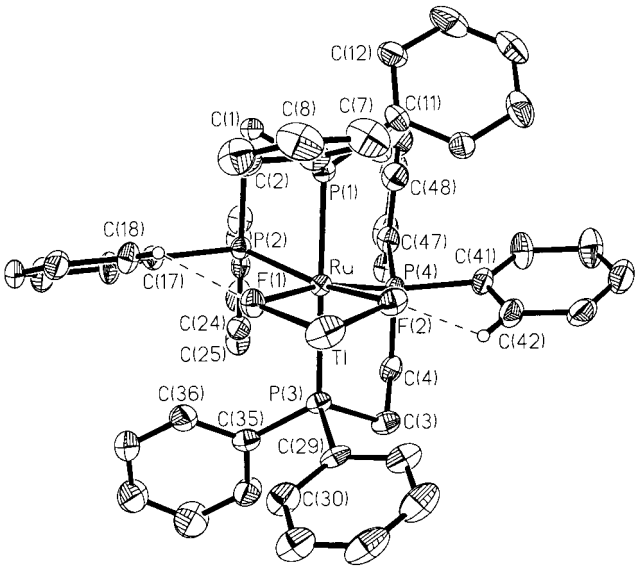

Figure 1. ORTEP view of [Ru(dppe)$_2$(μ-F)$_2$Tl]$^+$ (**9**) (30% probability ellipsoids).

Table 3. Selected Bond Distances (Å) and Angles (deg) for [Tl(μ-F)$_2$Ru(dppe)$_2$]PF$_6$ (9)

Tl(1)−F(1)	2.419(7)	Tl(1)−F(2)	2.419(8)
F(1)−Ru(1)	2.112(7)	F(2)−Ru(1)	2.119(7)
Ru(1)−P(1)	2.351(3)	Ru(1)−P(2)	2.306(3)
Ru(1)−P(3)	2.363(3)	Ru(1)−P(4)	2.299(3)
F(1)···H(18)	2.18	F(2)···H(42)	2.29
F(1)−Tl(1)−F(2)	66.7(2)	F(1)−Ru(1)−F(2)	77.9(3)
Ru(1)−F(1)−Tl(1)	107.8(3)	Ru(1)−F(2)−Tl(1)	107.5(3)
F(1)−Ru(1)−P(1)	85.9(2)	F(2)−Ru(1)−P(1)	84.2(2)
F(1)−Ru(1)−P(2)	95.5(2)	F(2)−Ru(1)−P(2)	166.7(2)
F(1)−Ru(1)−P(3)	84.9(2)	F(2)−Ru(1)−P(3)	86.2(2)
F(1)−Ru(1)−P(4)	168.0(2)	F(2)−Ru(1)−P(4)	97.0(2)
P(1)−Ru(1)−P(2)	83.80(9)	P(1)−Ru(1)−P(3)	167.9(1)
P(1)−Ru(1)−P(4)	104.6(1)	P(2)−Ru(1)−P(3)	104.9(1)
P(2)−Ru(1)−P(4)	91.5(1)	P(3)−Ru(1)−P(4)	83.9(1)
F(1)···H(18)−C(18)	138.4	F(2)···H(42)−C(42)	133.4

bond lengths are significantly longer in **9** (average 2.12 Å) than in the closely related *cis*-[RuF$_2$(dppp)$_2$] (average 2.06 Å),[8b] as expected on going from terminal to bridged fluorides. The Tl−F distances (both 2.42 Å) can only be compared to that in a Tl(III) fluoro porphyrin (2.441(6) Å),[14] as no other Tl^{I}−F distances are known. Despite the presence of the (μ-F)$_2$ bridge, the F(1)−Ru−F(2) angle in **9** (77.9(3)°) is similar to that in *cis*-[RuF$_2$-(dppp)$_2$] (78.2(1)°). The closest nonbonded contacts of the Tl atom are in the range 3.30(2)−3.79(2) Å and involve the carbon atoms of the axial phenyl rings (C(5)−C(10) and C(29)−C(34)), which form a pocket around the RuF$_2$ fragment. The closest F atom of the [PF$_6$]$^-$ anion, F(4), is 3.96(2) Å away from Tl.

Further features of **9** are the short H···F nonbonded contacts between the fluoro ligands and the ortho H atoms of both equatorial phenyl rings (Figure 1). The shortest F···H distances (based on idealized H positions with C−H = 1.00 Å) are 2.18 and 2.29 Å, which is significantly shorter than the sum of the van der Waals radii of F and H (ca. 2.7 Å) (Table 3). Similar contacts have been already observed in fluoro complexes of ruthenium and have been attributed to C−H···F hydrogen bonds.[8b,15] Complexes containing Ru−X−Tl linkages (X = halide) are very rare,[16] and to the best of our knowledge, **9** is the first μ-fluoro-bridged Tl adduct of a transition metal reported so far.

Scheme 3

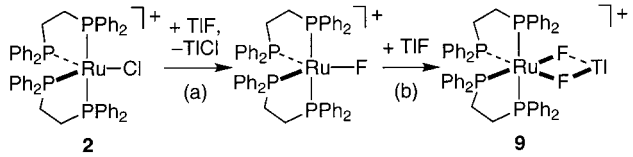

It should be noted that the reaction of the dppp analogue [RuCl(dppp)$_2$]$^+$ (**1b**) with TlF gives quantitatively the dark red, five-coordinate species [RuF(dppp)$_2$]$^+$ (**1a**) instead of a thallium adduct.[8] We suggest that this is because the dppp ligand is bulkier than dppe, which stabilizes a coordinatively unsaturated species.[17] In contrast, the hypothetical [RuF(dppe)]$^+$ is less stable, and its TlF adduct **9** is formed instead. In support of this interpretation, the reaction of [RuCl(dppe)$_2$]$^+$ (**2**) with 1 equiv of TlF yields **9** in 50% yield and unreacted **2** (50% of starting), which supports the stepwise reaction shown in Scheme 3.

The reactivities of complexes **9** and **1a** with alkyl bromides or iodides are completely analogous. Indeed, the reaction of the thallium adduct **9** with Ph$_3$C−Cl (2 equiv) gives Ph$_3$C−F and [RuCl(dppe)$_2$]PF$_6$ in nearly quantitative yield within 12 h. Also, **9** reacts with 1,3-diphenylallyl bromide or *tert*-butyl iodide to give the fluoro alkyl and [RuX(dppe)$_2$]$^+$ quantitatively after 24 h of reaction time.[18] As stated above, complex **9** is the only phosphine-containing species observed in solution by ^{31}P NMR spectroscopy during the catalytic fluorination. Similarly, the reaction solutions containing [RuCl(chiraphos)$_2$]PF$_6$ (**3**) as catalyst are yellow, and their ^{31}P NMR spectra suggest that [Tl(μ-F)$_2$Ru(chiraphos)$_2$]PF$_6$ is present. In contrast, the reaction solutions of dppp derivative **1b** are dark red during catalysis, which suggests that [RuF(dppp)$_2$]$^+$ is the main species in solution.

Conclusion

The observation of enantioselection, albeit at a low level, in the reaction of PhCHBr in the presence of the chiral complex **4** strongly supports the involvement of the metal complex in the reaction. The stoichiometric reactions indicate that both [RuF(P−P)$_2$]$^+$ and [Tl(μ-F)$_2$Ru(P−P)$_2$]$^+$ react with alkyl halides. At this stage, we cannot conclude which of these two species is the

(14) Coutsolelos, A. G.; Orfanopoulos, M.; Ward, D. L. *Polyhedron* **1991**, *10*, 885.

(15) (a) Coleman, K. S.; Fawcett, J.; Holloway, J. H.; Hope, E. G.; Russell, D. R. *J. Chem. Soc., Dalton Trans.* **1997**, 3557. (b) Cockman, R. W.; Ebsworth, E. A. V.; Holloway, J. H.; Murdoch, H.; Robertson, N.; Watson, P. G.; In *Inorganic Fluorine Chemistry*; Thrasher, J. S., Strauss, S. H., Eds.; ACS Symposium Series 555; American Chemical Society: Washington, DC, 1994.

(16) (a) Bianchini, C.; Masi, D.; Linn, K.; Mealli, C.; Peruzzini, M.; Zanobini, F. *Inorg. Chem.* **1992**, *31*, 4036. (b) Blake, A. J.; Christie, R. M.; Roberts, Y. V.; Sullivan, M. J.; Schröder, M.; Yellowlees, L. J. *J. Chem. Soc., Chem. Commun.* **1992**, 848. (c) Kahwa, I. A.; Miller, D.; Mitchel, M.; Fronczek, F. R.; Goodrich, R. G.; Williams, D. J.; O'Mahoney, C. A.; Slawin, A. M. Z.; Ley, S. V.; Groombridge, C. J. *Inorg. Chem.* **1992**, *31*, 3963.

(17) For a discussion of the effects that stabilize the five-coordinate species [RuX(dppe)$_2$]$^+$ (X = Cl, Br, I) and [RuX(dppp)$_2$]$^+$ (X = F, Cl, Br, I), see: Barthazy, P.; Broggini, D.; Mezzetti, A. *Can. J. Chem.* **2001**, *79*, 904.

(18) This protocol yields bromo and iodo complexes of the type [RuX(P−P)$_2$]$^+$ (X = Br, I), avoiding anion metathesis (often an untidy reaction). For an application, see ref 17.

Chart 2

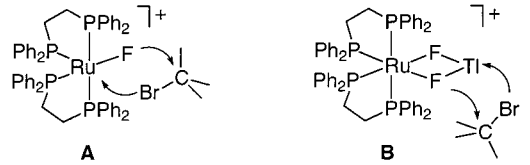

A **B**

active catalyst. If step b in Scheme 3 is reversible, both **1a** and **9** could react with R−X via the common intermediate $[RuFL_4]^+$ by elimination of TlF from **9**. We speculate that the 16-electron species $[RuFL_4]^+$ acts as a Lewis acid and interacts with the alkyl halide R−F. Indeed, electron-deficient (14- or 16-electron) complexes are known to form adducts with dichloromethane.[19] Coordination to the metal center could increase the polarization of the C−X bond and promote the σ-bond metathesis as sketched in **A** (Chart 2). Alternatively, the five-coordinate ruthenium complex could act merely as a shuttle of TlF in the organic solvent. The (soluble) thallium adduct $[Tl(\mu\text{-}F)_2Ru(P-P)_2]^+$ could then act as chloride scavenger and fluoride source as shown in **B** (Chart 2). However, the X-ray structure of **9** suggests that the Lewis acidity of the F-coordinated Tl^+ ion is low, as there are no close contacts to any other atom except to the fluoro ligands (and two phenyl protons, as discussed above). The latter observation somewhat disfavors the hypothetical intermediacy of **B** in the fluoride transfer as compared to **A** (Chart 2).[20] Finally, we explicitly stress that the pictorial descriptions in Chart 2 are merely working hypotheses and do not imply yet a mechanistic interpretation.

We have demonstrated the catalytic halide exchange for selective nucleophilic fluorination of moderately activated organic bromides and iodides by five-coordinate ruthenium(II) complexes. The present reaction opens the way to enantioselective nucleophilic fluorination. TlBr (or TlI) can be recycled. However, to avoid the use of the toxic and expensive TlF, we are investigating the use of different inorganic fluoride sources, as well as studying the mechanistic aspects of the X/F exchange, including the mechanism of enantioselection.

Experimental Section

General Considerations. All operations were carried out under argon using standard Schlenk techniques or in a glovebox (Braun AG) under purified nitrogen. All reagents and solvents were Fluka purissimum grade or had comparable purity. Solvents (including deuterated ones for NMR spectroscopy) and liquid reagents were distilled before use and/or dried over molecular sieves. As a variation of the published procedure,[10] $[RuCl(dppe)_2]PF_6$ was prepared by reacting *trans*-$[RuCl_2(dppe)_2]$[21] with $TlPF_6$. The NMR spectra were recorded on Bruker Avance 250 (for ^1H (250 MHz), ^{31}P (101 MHz), and Tl (144 MHz)) and 300 (^{19}F, 282 MHz) spectrometers. Chemical shifts δ are in ppm relative to internal $SiMe_4$ (^1H), to external 85% H_3PO_4 (^{31}P), to external $[Tl(OH_2)_6]^+$ (Tl), and to external $CFCl_3$ (^{19}F). FAB mass spectra were measured by the analytical service of Laboratorium für Organische Chemie of the ETH Zürich on a ZAB VSEQ instrument. The stoichiometric reactions of complex **9** with Ph_3C-Cl, 1,3-diphenylallyl bromide, and *tert*-butyl iodide were carried out and quantified as described in ref 8b.

Catalytic Fluorination (Method A). TlF (33 mg, 150 μmol) was suspended in a solution of the organic substrate (100 μmol) and the catalyst (10 μmol) in $CDCl_3$ (0.4 mL) in a Young NMR tube fitted with a Teflon liner. The NMR tube was shaken mechanically at room temperature. Products were identified by comparison of ^1H and ^{19}F NMR data with literature values and quantified by integration of the ^1H NMR spectra of the reaction solutions. Complex **4** was prepared in situ from $[RuCl_2(PNNP)]$ and $TlPF_6$ as previously reported.[9c]

Reaction with *tert*-Butyl Bromide (5c). ^1H NMR ($CDCl_3$): δ 1.83 (s, 9H, $C(CH_3)_3$, **5c**); 1.38 (lit.[22] 1.30, d, 9H, $J_{F,H} = 21.1$ Hz, lit. 20,[22] $F-C(CH_3)_3$, **5a**); 4.66 (lit.[23] 4.55, m, 2H, $(CH_3)C{=}CH_2$)); 1.75 (t, 6H, $J_{H,H} = 1$ Hz, $(CH_3)C{=}CH_2$)); 1.28 (lit.[24] 1.27, s, $(CH_3)_3COC(CH_3)_3$). ^{19}F NMR ($CDCl_3$): δ −131.0 (lit.[25] −132, 10 lines, 1F, $J_{F,H} = 21.1$ Hz, lit.[25] 21, C−*F*, **5a**).

Reaction with *tert*-Butyl Iodide (5d). ^1H NMR ($CDCl_3$): δ 1.95 (s, 9H, $C(CH_3)_3$, **5d**), data for **5a** are as reported above for **5c**.

Reaction with 6c. ^1H NMR ($CDCl_3$): δ 6.31 (s, 1H, CBr−*H*, **6c**); 6.48 (d, 1H, $J_{F,H} = 47.8$ Hz, $Ph_2C(F)-H$, **6a**); 5.40 (lit.[26] 5.38, s, 1H, $Ph_2CHOC(H)Ph_2$). ^{19}F NMR ($CDCl_3$): δ −166.9 (lit.[25] −169, d, 1F, $J_{F,H} = 46.6$ Hz, lit.[25] 48, $Ph_2C(H)-F$, **6a**).

Reaction with 7c. ^1H NMR ($CDCl_3$): **7c**: δ 7.26−7.47 (lit. 7.35, m, 5H, arom), 5.23 (lit. 5.22, q, 1H, $J_{H,H} = 6.9$ Hz, CBr−*H*), 2.06 (lit. 2.0, d, 3H, $J_{H,H} = 6.9$ Hz, CH_3).[27] **7a**: ^1H NMR ($CDCl_3$): δ 7.18−7.40 (lit. 7.45, m, 5H, arom), 5.64 (lit. 5.55, dq, 1H, $J_{H,H} = 6.4$ Hz, $J_{F,H} = 47.6$ Hz, CF−*H*), 1.66 (lit. 1.60, 3H, dd, $J_{H,H} = 6.4$ Hz, $J_{F,H} = 23.9$ Hz, CH_3).[28] ^{19}F NMR ($CDCl_3$): δ −167.4 (lit. −167.5, sextet, 1F, $^3J_{F,H} = 24$ Hz, lit. 24 Hz, $^2J_{F,H} = 48$ Hz, lit. 48 Hz, C−*F*, **7a**).[28]

Reaction with 8c. ^1H NMR ($CDCl_3$): **8c**: δ 7.12−7.35 (m, 4H, arom), 5.66 (s, 1H, C(1)−*H*), 4.95 (s, 1H, C(2)−*H*), 3.21−3.36 (m, 1H, CH_2), 2.76−3.08 (m, 2H, CH_2), 2.15−2.23 (m, 1H, CH_2). **8a**: ^1H NMR ($CDCl_3$): δ 7.14−7.45 (lit. 7.1−7.4, m, 4H, arom), 5.62 (lit. 5.58, dd, 1H, $J_{H,H} = 5$ Hz, $J_{F,H} = 51$ Hz, CF−*H*), 4.61 (lit. 4.55, m, 1H, CBr−*H*), 2.65−3.35 (lit. 2.6−3.2, 2H, m, CH_2), 2.12−2.62 (lit. 2.0−2.6, 2H, m, CH_2).[29] ^{19}F NMR ($CDCl_3$): δ −145.2 (lit.[29] −146.0, doublet, 1F, $^2J_{F,H} = 51$ Hz, C−*F*, **8a**).

Catalytic Fluorination of 6a (Method B). All manipulations were performed in a glovebox to exclude rigorously traces of moisture. TlF (1.1 mmol) was added to a solution of **7c** (1 mmol), decane (as internal standard), and the catalyst (10 μmol) in CH_2Cl_2 (5 mL) in a 15 mL Teflon vessel fitted with a Teflon-coated magnetic bar. The suspension was stirred at

(19) For examples of complexes containing coordinated chloro alkanes that are not stabilized by the chelate effects, see: (a) Fang, X. G.; Scott, B. L.; John, K. D.; Kubas, G. J. *Organometallics* **2000**, *19*, 4141. (b) Huhmann-Vincent, J.; Scott, B. L.; Kubas, G. J. *Inorg. Chem.* **1999**, *38*, 115. (c) Huhmann-Vincent, J.; Scott, B. L.; Kubas, G. J. *J. Am. Chem. Soc.* **1998**, *120*, 6808. (d) Huang, D.; Huffman, J. C.; Bollinger, J. C.; Eisenstein, O.; Caulton, K. G. *J. Am. Chem. Soc.* **1997**, *119*, 7398. For a recent example of Ag-coordinated CH_2Cl_2, see: Forniés, J.; Martínez, F.; Navarro, R.; Urriolabeitia, E. P. *Organometallics* **1996**, *15*, 1813.

(20) We thank one of the reviewers for this suggestion and for the observation that the fluoro ligand in **9** could deprotonate Bu^t-X in view of its high basicity. However, we expect that the coordination to thallium strongly decreases the basicity of fluoride, which also explains the stability of the thallium adduct itself.

(21) Chatt, J.; Hayter, R. G. *J. Chem. Soc.* **1961**, 896.

(22) Olah, G. A.; Baker, E. B.; Evans, J. C.; Tolgyesi, W. S.; McIntyre, J. S.; Bastien, I. J. *J. Am. Chem. Soc.* **1964**, *86*, 1360.

(23) White, E. H.; Reefer, J.; Erickson, R. H.; Dzadzic, P. M. *J. Org. Chem.* **1984**, *49*, 4872.

(24) King, J. F.; Lam, J. Y. L.; Dave, V. *J. Org. Chem.* **1995**, *60*, 2831.

(25) Lai, C.; Kim, Y. I.; Wang, C. M.; Mallouk, T. E.; *J. Org. Chem.* **1993**, *58*, 1393.

(26) Mizuno, H.; Matsuda, M.; Iino, M. *J. Org. Chem.* **1981**, *46*, 520.

(27) Venkatachalapathy, C.; Pitchumani, K. *Tetrahedron* **1997**, *53*, 2581.

(28) York, C.; Surya Prakash, G. K.; Olah, G. A.; *Tetrahedron* **1996**, *52*, 9.

(29) Shimizu, M.; Nakahara, Y.; Yoshioka, H. *J. Chem. Soc., Chem. Commun.* **1989**, 1881.

room temperature. Reaction control was performed by ^{1}H, ^{31}P, and ^{19}F NMR and gas chromatography. Spectroscopic data for **7a** were identical with those in the literature. Relevant features of ^{1}H and ^{19}F NMR spectra of the reaction solutions and reference to the literature are given above. The reactions were quantified by gas chromatography on a Fisons Instruments GC 8000 gas chromatograph equipped with an Optima δ-3 capillary column (30 m × 0.25 mm, 0.25 μm film) and on a ThermoQuest Trace GC 2000 Series gas chromatograph equipped with a Supelco Beta Dex capillary column (30 m × 0.25 mm, 0.25 μm film). FID detectors were used for signal detection on both chromatographs. Quantitative analyses were performed using *n*-decane as internal standard. Response factor R_f (1.75) of 1-bromo-1-phenylethane (**7c**) was determined by injection of a solution of **7c** and decane of known concentration. The response factor of **7a** was determined by comparison of the area of the product with the integrated intensities from a one-pulse ^{1}H NMR spectrum of the same solution (δ 1.24 for 1-fluoro-1-phenylethane, **7a**). The temperature program used for achiral GC analysis was a 5 min isotherm 50 °C, then 5 °C/min until 200 °C. Retention times were 10.8 min for 1-fluoro-1-phenylethane (**7a**), 14.3 min for decane, and 19.7 min for 1-bromo-1-phenylethane (**7c**). The temperature program used for chiral GC was isotherm (50 °C). The retention time for **7a** was 43.3 min for the first enantiomer and 46.9 min for the second one.

[Tl(μ-F)$_2$Ru(dppe)$_2$]PF$_6$ (9). A CH_2Cl_2 suspension (30 mL) of [RuCl(dppe)$_2$]PF$_6$ (1.134 g, 1.05 mmol) and TlF (530 mg, 2.38 mmol) was stirred for 3 h at room temperature. The thallium salts were filtered off, and the solution was transferred dropwise into hexane (100 mL) with vigorous stirring. The light yellow precipitate was filtered off and dried under vacuum: 1.095 g (81%). ^{1}H NMR ($CDCl_3$): δ 7.9−8.0 (m, br, 4H, Ph *H*), 7.6−7.7 (m, 8H, Ph *H*), 7.4−7.5 (m, 8H, Ph*H*), 7.38 (t, 6H, Ph *H*, $J_{H,H}$ = 7.3 Hz), 7.28 (t, 2H, Ph *H*, $J_{H,H}$ = 7.4 Hz), 7.07 (t, 4H, Ph *H*, $J_{H,H}$ = 7.6 Hz), 6.86 (t, 4H, Ph *H*, $J_{H,H}$ = 7.6 Hz), 5.86 (t, 4H, Ph *H*, $J_{H,H}$ = 8.1 Hz), 3.0−3.2 (m, 2H, PCH_2), 2.2−2.4 (m, 4H, PCH_2), 1.6−1.8 (m, 2H, PCH_2). ^{31}P NMR (CD_2Cl_2, 183 K): δ 55.7 (*pseudo*-quintet, 2P, $J_{P,P'} \cong$ 19 Hz, $J_{P,F'} \cong$ 19 Hz, P_{ax}), 54.4 (d × t, 2P, $J_{P,P'} \cong$ 19 Hz, $J_{P,F'} \cong$ 145 Hz, P_{eq}), −143.1 (septet, 1P, PF_6, $J_{P,F}$ = 710 Hz). ^{19}F NMR ($CDCl_3$, 293 K): δ 74.5 (d, 6F, $J_{P,F}$ = 710 Hz, PF_6), −296 (br d, 2F, $J_{Tl,F}$ = 800 Hz, RuF_2). ^{205}Tl NMR ($CDCl_3$, 293 K): δ 1055 (br t, 1Tl, $J_{Tl,F}$ = 800 Hz, F_2*Tl*). MS (FAB$^+$) *m*/*z*: 1141 ([M]$^+$, 12%), 917 ([M − TlF]$^+$, 16%), 899 ([RuH(dppe)$_2$]$^+$, 100%), 499 ([RuH(dppe)]$^+$, 5%). Anal. Calcd for $C_{52}H_{48}F_8P_5RuTl$: C, 48.59; H, 3.76. Found: C, 48.71; H, 3.78.

X-ray Structure Determination of [Tl(μ-F)$_2$Ru(dppe)$_2$] (9). Crystals were obtained by diffusion of hexane into a CH_2Cl_2 solution of **9** at room temperature. Crystal data: $C_{52}H_{48}F_8P_5RuTl$, yellow prism, M_r = 1285.19, T = 293 K, triclinic, $P\bar{1}$, a = 10.7584(3) Å, b = 11.1670(3) Å, c = 11.7810(2) Å, α = 74.980(1)°, β = 63.60°, γ = 87.030(1)°, V = 1221.09(5) Å^3, $F(000)$ = 632, Z = 1, D_c = 1.748 Mg m^{-3}, μ(Mo Kα) = 3.835 mm^{-1}, crystal size 0.40 × 0.38 × 0.22 mm^3, Siemens SMART platform with CCD detector, normal focus molybdenum-target X-ray tube, graphite monochromator, ω-scans, h = −13 to +14, k = −14 to +14, l = −11 to +15; 8998 reflections for 1.89° < θ < 30.01° (7135 unique). Unit cell dimension determination and data reduction were performed by standard procedures, and an empirical absorption correction (SADABS) was applied. The structure was solved with SHELXS-96 using direct methods and refined by full-matrix least squares on F^2 with anisotropic displacement parameters for all non-H atoms. The crystal is a 50:50 racemic twin, and the absolute structure parameter was 0.465(8). Hydrogen atoms were introduced at calculated positions and refined with the riding model and individual isotropic thermal parameters. R1 = 0.0522 and wR2 = 0.1256 (6430 unique reflections with $I > 2\sigma(I)$), R1 = 0.0634, and wR2 = 0.1401 (all data), GOF = 1.172. The maximum and minimum difference peaks were 1.651 and −1.300 e Å^{-3}, and the largest and mean values of Δ/σ were 0.063 and 0.02. Selected bond lengths and angles are given in Table 3. Atomic coordinates, anisotropic displacement coefficients, and an extended list of interatomic distances and angles are available as Supporting Information.

Acknowledgment. This work was supported by the ETH Zürich. We thank Dr. H. Rüegger for assistance with the ^{19}F and ^{205}Tl NMR spectra and D. Broggini and Dr. M. Wörle for the X-ray crystallographic study.

Supporting Information Available: Details of the X-ray study of **9**. This material is available free of charge via the Internet at http://pubs.acs.org.

OM010288G